Theoretical Microfluidics

MICRO-718

T. Lehnert and M.A.M. Gijs (EPFL-LMIS2)

EPFL - Lausanne

Doctoral Program in Microsystems and Microelectronics (EDMI)

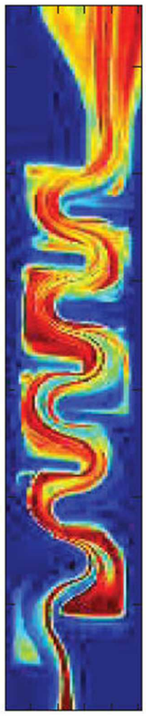

3. Microfluidic channels and circuits

3.1 Poiseuille flow in channels with different cross-sections

3.2 Hydraulic resistance and microfluidic networks

3.3 Compliance (hydraulic capacitance)

3.4 Microfluidic devices based on elastomeric components

3.1 Poiseuille flow

In 1839, Hagen corrected an older formula for the hydraulic resistance of a pipe and introduced the $\boldsymbol{Q \sim \Delta p \cdot d^4}$ relationship for the flow rate Q, including also a Q^2 term.

$$\Delta p = \frac{1}{d^4}\left(aLQ + bQ^2\right)$$

$$Q = K'' \frac{d^4}{L} \Delta p$$

Poiseuille's interest in hemodynamics led him to undertake extensive studies of liquid (laminar) flow in glass tubes and capillaries. He found that only the first term **~*Q*** was valid in this case.

Further reading: **THE HISTORY OF POISEUILLE'S LAW**
S.P. Sutera and R. Skalak
Annu. Rev. Fluid Mech. 25: 1-19 (1993)

In 1839, Poiseuille deposited with the *French Academy of Sciences* a sealed packet containing the results of his studies. It actually appeared in the *Mémoires Presentés par Divers Savants à l'Academie Royale des Sciences de l'Institut de France* in 1846, seven full years after he delivered his first sealed packet to the Academy.

$$Q = K''PD^4/L$$

K" being simply a function of temperature and the type of liquid flowing.

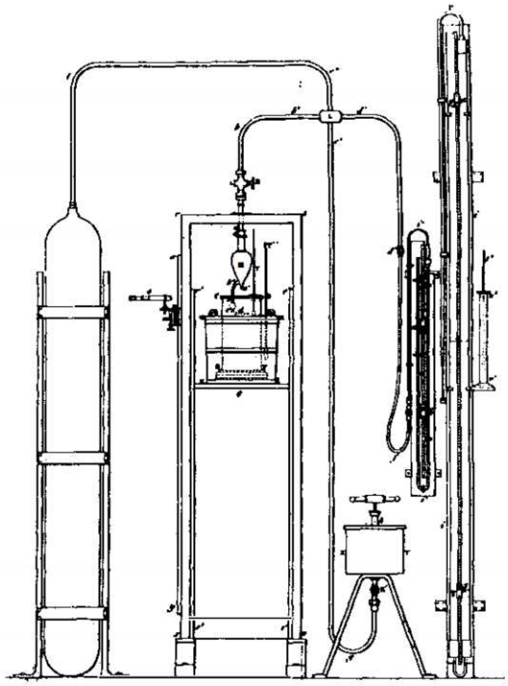

Figure 1 Frontal elevation view of Poiseuille's apparatus. Photocopy of one segment of a ten part fold-out plate published with Poiseuille's summary paper (1846).

Pressure-driven laminar flow between infinite parallel plates

Applicable for long rectangular channels with high aspect ratio ($w/h >> 1$, translation invariance in x and y direction). The flow is induced by a constant positive pressure difference Δp over a length L.

$$p(\mathbf{r}) = \frac{\Delta p}{L}\,(L - x) + p_0 \qquad (3.19)$$

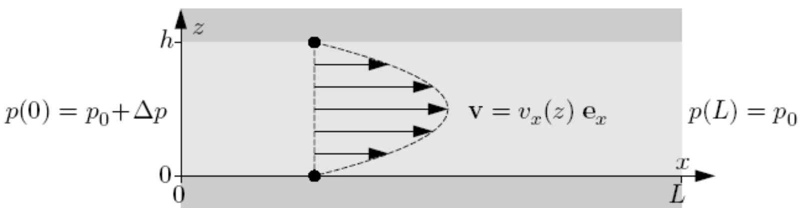

(Fig. 3.6)

Navier-Stokes eqn.

$$\boxed{\partial_z^2 v_x(z) = -\frac{\Delta p}{\eta L}} \qquad \begin{aligned} v_x(0) &= 0, && \text{(no-slip)} \\ v_x(h) &= 0, && \text{(no-slip)} \end{aligned} \qquad (3.28)$$

⇨ **Parabolic flow profile**

$$\boxed{v_x(z) = \frac{\Delta p}{2\eta L}\,(h - z)z} \qquad (3.29)$$

⇨ Flow rate (channel w, h, L)

$$\boxed{Q = \int_0^w \mathrm{d}y \int_0^h \mathrm{d}z\, \frac{\Delta p}{2\eta L}\,(h - z)z = \frac{h^3 w}{12\eta L}\,\Delta p} \qquad (3.30)$$

(3.30) can be used as approximation for real channels:
error 23% for $w/h = 3$ and 7% for $w/h = 10$

Hele-Shaw flow patterns between parallel plates

Hele-Shaw cell: bounded flow between two parallel plates separated by a distance h (z-direction) much smaller than (x,y) dimensions in the plane.

Examples: Wide and shallow microchannels or a chamber with cylindrical spacers ($Re << 1$)

⇨ $p(z) \approx$ const and $p = p(x,y)$ ⇨ Variables can be separated in the Stokes equation (2.41).

Hele-Shaw solution for the flow field

$$\mathbf{v} = -\frac{1}{2\eta} z(h-z)\nabla p$$

The flow profile in z-direction is parabolic.

The flow in the (x,y) plane can be considered as a 2D potential flow (no z voritcity). A Laplace eqn for $p(x,y)$ has to be solved and $\mathbf{v}(x,y)$ can be calculated.

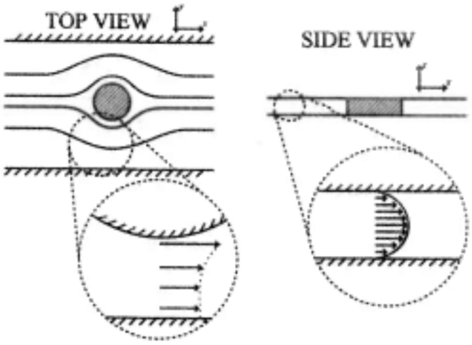

Hele-Shaw flow around a circular spacer. The velocity field in (x,y) plane (top view) appears as a potential flow in all regions at a distance from the side walls that is large relative to the depth of the channel.

Poiseuille flow in channels with rectangular cross-section

More details in *Henrik Bruus* "Theoretical Microfluidics"

$$\boxed{[\partial_y^2 + \partial_z^2] v_x(y,z) = -\frac{\Delta p}{\eta L}} \qquad \text{for} \quad -\frac{1}{2}w < y < \frac{1}{2}w, \quad 0 < z < h$$

$$v_x(y,z) = 0, \qquad \text{for} \quad y = \pm\frac{1}{2}w, \; z = 0, \; z = h. \tag{3.47}$$

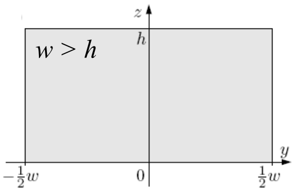

⇨ No analytical solution is known ! Solution may be expressed as Fourier series :

$$v_x(y,z) \equiv \sum_{n=1}^{\infty} f_n(y) \sin\left(n\pi\frac{z}{h}\right) \quad \text{and} \quad -\frac{\Delta p}{\eta L} = -\frac{\Delta p}{\eta L}\frac{4}{\pi}\sum_{n,\text{odd}}^{\infty}\frac{1}{n}\sin\left(n\pi\frac{z}{h}\right)$$

in (3.47)

$$[\partial_y^2 + \partial_z^2] v_x(y,z) = \sum_{n=1}^{\infty}\left[f_n''(y) - \frac{n^2\pi^2}{h^2} f_n(y)\right] \sin\left(n\pi\frac{z}{h}\right) \tag{3.50}$$

Coefficients have to be found:

$$\begin{aligned} f_n(y) &= 0, && \text{for } n \text{ even}, \\ f_n''(y) - \frac{n^2\pi^2}{h^2} f_n(y) &= -\frac{\Delta p}{\eta L}\frac{4}{\pi}\frac{1}{n}, && \text{for } n \text{ odd}. \end{aligned} \tag{3.51}$$

EPFL

⇨ Velocity profile in a rectangular channel

$$v_x(y,z) = \frac{4h^2\Delta p}{\pi^3 \eta L} \sum_{n,\mathrm{odd}}^{\infty} \frac{1}{n^3}\left[1 - \frac{\cosh\left(n\pi\frac{y}{h}\right)}{\cosh\left(n\pi\frac{w}{2h}\right)}\right] \sin\left(n\pi\frac{z}{h}\right) \tag{3.56}$$

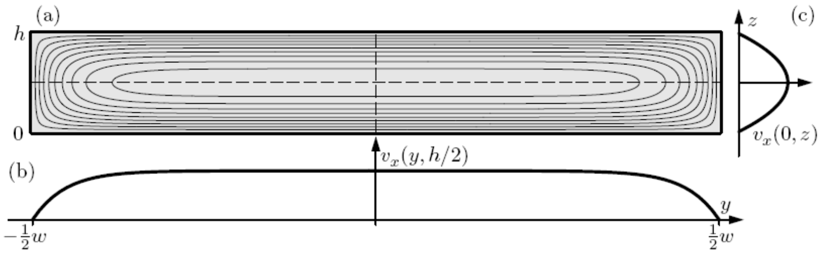

(Fig. 3.9)

(a): Contour lines for $v_x(y,z)$ in steps of 10% of $v_{x,max}$
(b) and (c): $v_x(y,h/2)$ and $v_x(0,z)$ along the respective centerlines.

⇨ Flow rate in a rectangular channel (approximation for $h/w \to 0$, $w > h$)

$$\boxed{Q = 2\int_0^{\frac{1}{2}w} \mathrm{d}y \int_0^h \mathrm{d}z\ v_x(y,z) \approx \frac{h^3 w \Delta p}{12\eta L}\left[1 - 0.630\,\frac{h}{w}\right]} \tag{3.58}$$

Good approximation ! Error 13% for $h = w$ and only 0.2% for $h = w/2$

EPFL

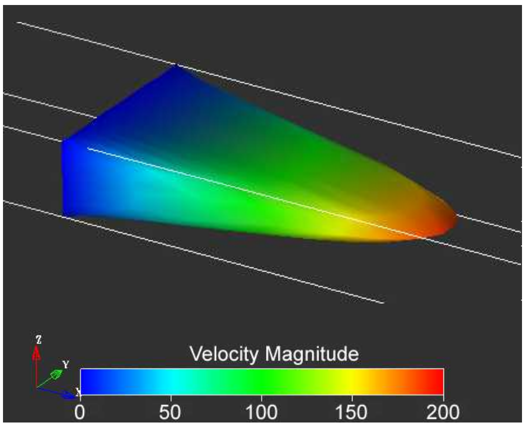

Parabolic velocity profile of a pressure driven laminar flow in a microchannel, assuming no-slip boundary condition (simulation, aspect ratio 2:5, velocity at the walls is zero).

http://faculty.washington.edu/yagerp/microfluidicstutorial/basicconcepts/basicconcepts.htm

$t < 0$, no flow, magnetic beads are retained in between two magnetic tips.

$t = 0$, the magnetic field is removed and flow starts (2 nL/s).

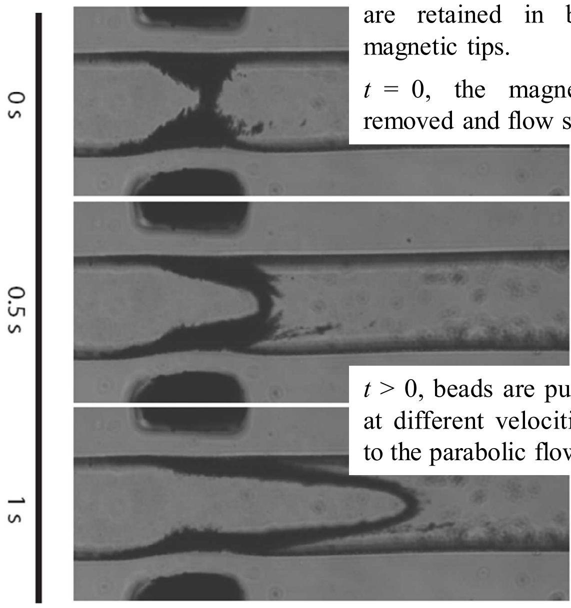

$t > 0$, beads are pushed forward at different velocities according to the parabolic flow profile.

Experimental: Visualization of a parabolic flow profile using a plug of magnetic microbeads in a microchannel (width 100 µm, Y. Moser, EPFL-LMIS2).

Flow in capillaries with circular cross-section

Navier-Stokes eqn. in cylindrical coordinates (r, θ, x) in a pipe with radius a (length L). A constant pressure drop Δp is applied along the x-direction. The flow profile is axisymmetric with respect to the center line (v_x is independent of θ). No-slip at the pipe wall ($r = a$).

$$\left[\partial_r^2 + \frac{1}{r}\,\partial_r\right] v_x(r) = -\frac{\Delta p}{\eta L} \qquad (3.39a)$$

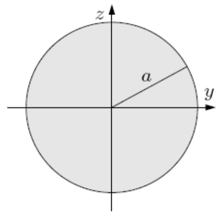

…using a trial solution $v_x(r) = v_0\,(1 - r^2/a^2)$

⇨ Velocity profile $v_x(r,\phi) = \dfrac{\Delta p}{4\eta L}\left(a^2 - r^2\right)$

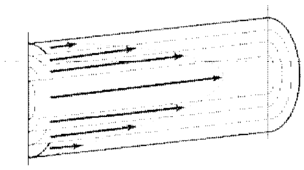

⇨ Flow rate (Hagen-Poiseuille law)

$$\boxed{Q = \frac{\pi a^4}{8\eta L}\,\Delta p} \qquad (3.42b)$$

Δp is the pressure difference
L is the length of pipe
η is the dynamic viscosity
Q is the volumetric flow rate
a is the pipe radius.

Flow rate for arbitrary cross-sections

- Navier-Stokes eqn. for the velocity field v_x in a channel with arbitrary cross-section

$$\boxed{\begin{aligned} \left[\partial_y^2 + \partial_z^2\right] v_x(y,z) &= -\frac{\Delta p}{\eta L}, \quad \text{for } (y,z) \in \mathcal{C} \\ v_x(y,z) &= 0, \qquad \text{for } (y,z) \in \partial\mathcal{C} \end{aligned}} \qquad (3.20)$$

- Flow rate Q through channel with cross-section C

Volumetric flow rate $\quad Q \equiv \int_{\mathcal{C}} \mathrm{d}y\,\mathrm{d}z\; v_x(y,z)$

Mass flow rate $\quad Q_{\text{mass}} \equiv \int_{\mathcal{C}} \mathrm{d}y\,\mathrm{d}z\; \rho\, v_x(y,z)$ (3.21)

- The flow rate/pressure dependence may be found by expansion of v_x

$$\boxed{Q \approx \frac{\Delta p}{2\eta L}\frac{A^3}{P^2}} \qquad (3.27)$$

⇒ Linear relationship with $R \approx A^3/(2hLP^2)$

where $\mathcal{A}$ is the cross-section area and $\mathcal{P}$ is the perimeter; hydrodynamic diameter $r \equiv 2\mathcal{A}/\mathcal{P}$

EPFL

3.2 Hydraulic resistance and microfluidic networks

The proportional constant in the linear relationship between pressure drop Δp and flow rate Q (Poiseuille flow) may be defined as the **hydraulic resistance R_{hyd}** (or inverse conductance G^{-1}_{hyd}).

$$\boxed{\Delta p = R_{\text{hyd}}\, Q = \frac{1}{G_{\text{hyd}}}\, Q}$$

Hagen-Poiseuille law

$$[Q] = \frac{\text{m}^3}{\text{s}} \qquad [\Delta p] = \text{Pa} = \frac{\text{N}}{\text{m}^2} = \frac{\text{kg}}{\text{m s}^2} \qquad [R_{\text{hyd}}] = \frac{\text{Pa s}}{\text{m}^3} = \frac{\text{kg}}{\text{m}^4\,\text{s}} \qquad (4.1)$$

⇨ The Hagen-Poiseuille law can be considered as fluidic analog to the Ohm's law ($I_{el} \rightarrow Q$; $V_{el} \rightarrow \Delta p$; $R_{\text{el}} \rightarrow R_{\text{hyd}}$). This "fluidic Ohm's law" for laminar flow conditions is of fundamental importance for the design of microfluidic circuits.

⇨ Further-going analogy:

Capacitance/Compliance: $C_{\text{el}} \rightarrow C_{\text{hyd}}$

Inductance/Inertia: $L_{\text{hyd}} = \rho L/A$

(relevant only for fluidic switching frequencies > 100 Hz and relative large/long channels (≥ mm-size).

⇨ The concept of impedance also applies, *e.g.* for an oscillating *p(t)* stimulus. **Equivalent electrical circuits** may be established to analyze the fluidic response of microfluidic circuits.

EPFL

Hydraulic resistances for Poiseuille flow straight channels with different cross-sections

(table 4.1)

shape		R_{hyd}	R_{hyd} $[10^{11}\ \frac{\text{Pa s}}{\text{m}^3}]$
circle		$\frac{8}{\pi}\eta L \frac{1}{a^4}$	0.25
two plates	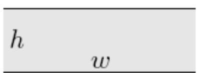	$12\,\eta L \frac{1}{h^3 w}$	0.40
rectangle	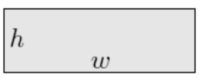	$\frac{12\,\eta L}{1-0.63(h/w)}\frac{1}{h^3 w}$	0.51
square	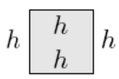	$\frac{12\,\eta L}{1-0.917\times 0.63}\frac{1}{h^4}$	2.84
arbitrary		$\approx 2\eta L\, \mathcal{P}^2/\mathcal{A}^3$	P perimeter; A cross section $2A/P \equiv$ hydraulic radius

Numerical values are for: water η = 1mPa·s, channel length L = 1 mm, a = 100 µm, b = 33 µm, h = 100 µm, w = 300 µm.

Fluidic "Kirchhoff laws" at low Re-numbers

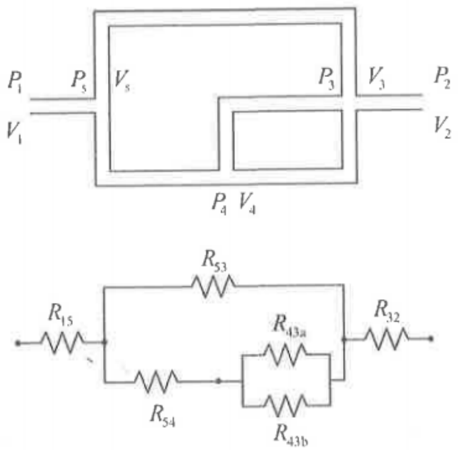

Hydraulic circuit analog of a simple microfluidic device.

1) The total pressure drop Δp_i in a closed loop is zero.

2) The sum of flow rates Q_i at a node is zero (conservation of mass).

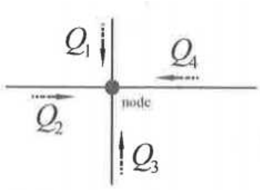

$$\Sigma Q = Q_1 + Q_2 + Q_3 + Q_4 = 0$$

R_{hyd} for a series connection of two channels ($\boldsymbol{\Delta p = \Sigma p_i}$)

$$\boxed{R = R_1 + R_2} \qquad (4.42)$$

R_{hyd} for a parallel connection of two channels ($\boldsymbol{Q = \Sigma Q_i}$)

$$\boxed{R = \left(\frac{1}{R_1} + \frac{1}{R_2}\right)^{-1}} \qquad (4.43)$$

Channels/parallel plates with a height step ($h_1 \rightarrow h_2$): Hagen-Poiseuille remains valid for each subsection (in general applicable for microfluidic systems if $L >> h$). Translational invariance is broken at the channel junction: $(\mathbf{v}\cdot\nabla)\,\mathbf{v} \neq 0$

a) $Re = 0.01$, the transition is smooth and happens on a length scale $< h_1$.

$$\Delta p \approx (R_1 + R_2)Q$$

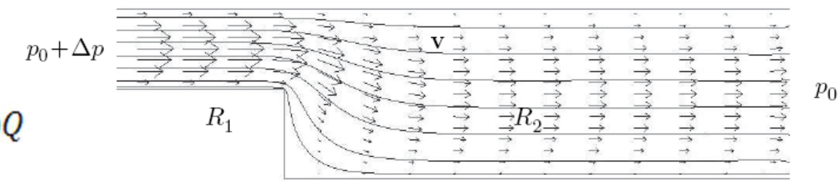

b) $Re = 100$, a convection roll appears at the step. The transition happens on a length scale $> h_1$. Hagen-Poiseuille can not be strictly applied.

$$\Delta p \neq (R_1 + R_2)Q$$

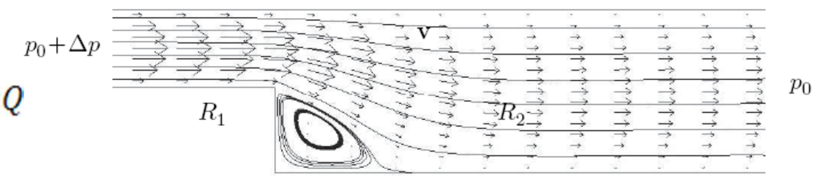

(Fig. 4.6)

Example 1: Hydrodynamic trapping of droplets

W. Shi et al, Lab Chip, 8, 1432-1435 (2008)

C. elegans worms are encapsulated in aqueous droplets and subsequently aligned on a microfluidic array. Droplet capture occurs by passive hydrodynamic trapping due to variations of the hydraulic channel resistances.

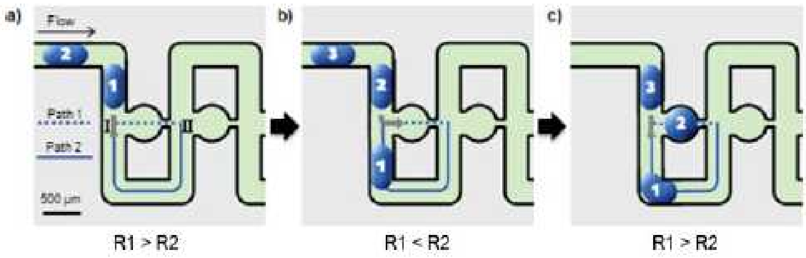

Process of droplet trapping in the array.

The flow resistances along the two paths from junction I to II (path 1, P1 and path 2, P2) are defined as R1 and R2, respectively. R1 > R2 for open channels.

Figure: (a) R1 > R2, droplet 1 at junction I will flow into P2; (b) R2 > R1, droplet 2 at junction I will flow into P1 and be trapped; (c) R1 > R2, droplet 3 will flow into P2 and enter the next trapping process.

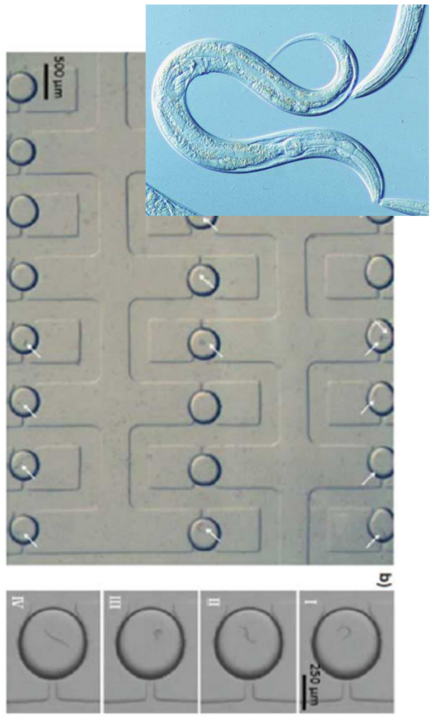

Array of 24 droplets with C. elegans worms

Example 2: Hydrodynamic filtration on-chip

M. Yamada et al, Lab Chip, 5, 1233-1239 (2005) and Anal. Chem., 78, 1357-1362 (2006)

Hydrodynamic filtration enables continuous concentration and classification of particles/cells in microfluidic devices. The flow ratios (hydraulic resistance ratios) in the channel network determine the filtered particle size. No accurate external flow control is required.

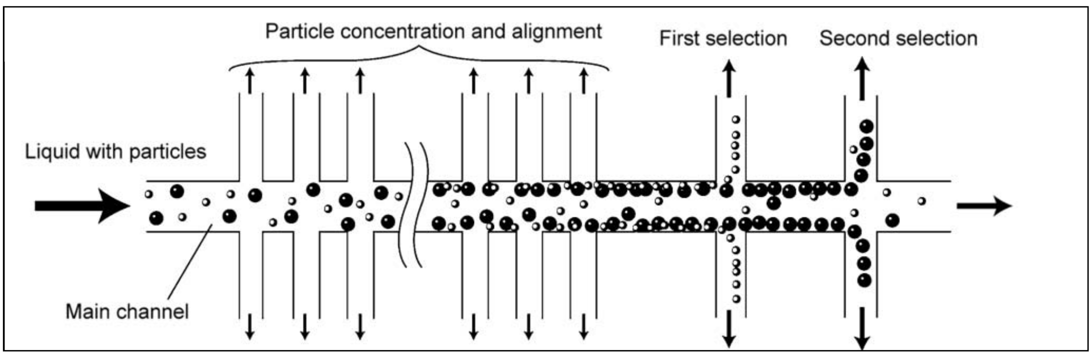

Principle of hydrodynamic filtration:

1) By withdrawing a small amount of liquid repeatedly from the main stream through the side channels, particles are first concentrated and aligned onto the sidewalls.

2) Further downstream, the relative flow rate at a branch point with a specific selection channel determines particle behavior and size-dependent separation.

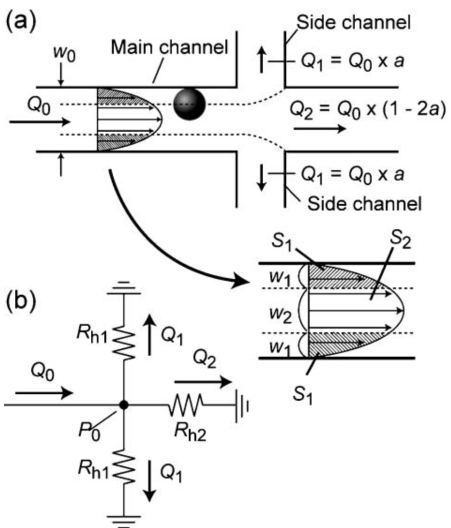

Relation between the channel geometry, filtered particle size and flow rate distribution. (a) Flow rate distribution at a branch point. (b) Diagram of a resistive circuit corresponding to the microchannel structure.

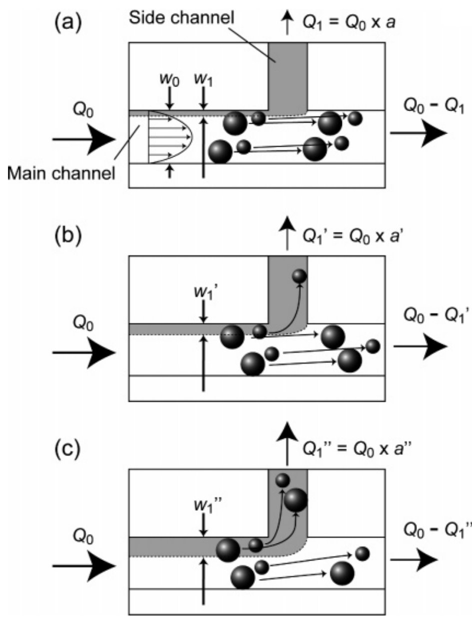

Relation between particle behavior and relative flow rate distributed into a side channel at a branch point. The relative flow rate into the side channel is (a) small, (b) medium, and (c) large, *i.e.* a < a′ < a″. The virtual region of the flow distributed into the side channel is dark-colored.

M. Yamada et al, Lab Chip, 5, 1233-1239 (2005) and Anal. Chem., 78, 1357-1362 (2006)

Application: Selective enrichment of leukocytes

Leukocytes are usually separated from blood by centrifugation. Conventional filtration methods cannot be applied.

⇨ **Hydrodynamic filtration on-chip** resulted in a ~29-fold increase of the relative leukocytes concentration (∅ > 8 μm) with respect to erythrocytes (2-3 μm, flat).

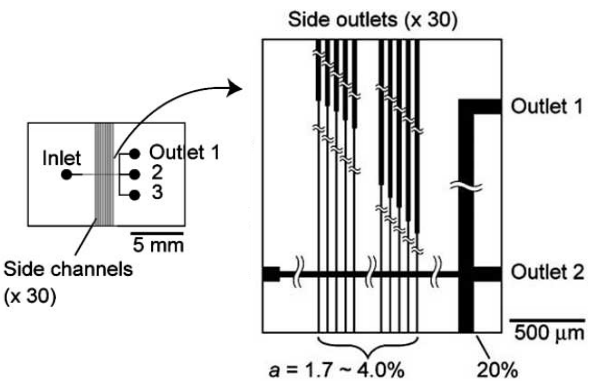

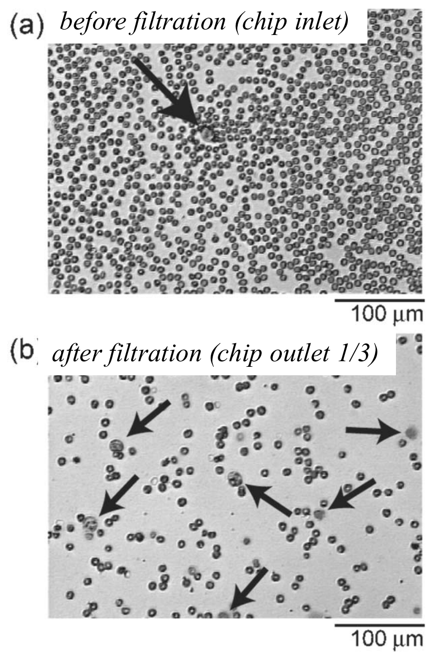

Microdevice for leukocyte enrichment (PDMS on glass): Main channel w_0 = 40 μm (depth 15 μm). Each side channel consists of narrow (w = 10 μm) and broad (w = 30 μm) segments (total length 5 mm). The flow width w_1 that is distributed into the side channels is 3.1 - 4.8 μm (a = 1.7 - 4.0%) and 11.4 μm (a = 20%) for outlet 1/3, respectively ⇨ Erythrocytes go through the side channels, while a large portion of leukocytes could be collected from outlets 1/3.

M. Yamada et al, Lab Chip, 5, 1233-1239 (2005) and Anal. Chem., 78, 1357-1362 (2006)

Example 3: Hydrodynamic focusing

R. Aoki et al., Microfluid Nanofluid, 6, 571-576 (2009)

Repeated flow splitting and re-injecting generates sheath flows for continuously focusing of particles. No extra flow or external control required ⇨ Flow cytometry on-chip.

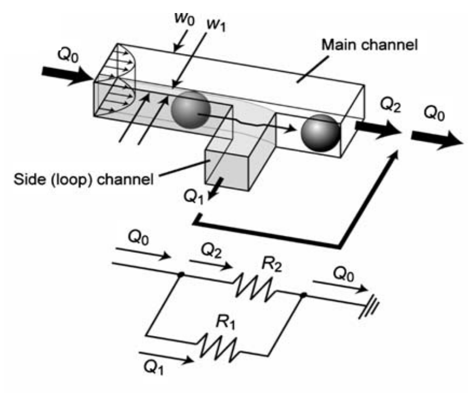

Branch point in the main channel. The flow section entering into the side channel is gray-colored. Particles do not enter. The corresponding resistive circuit consists of the main channel and a loop channel.

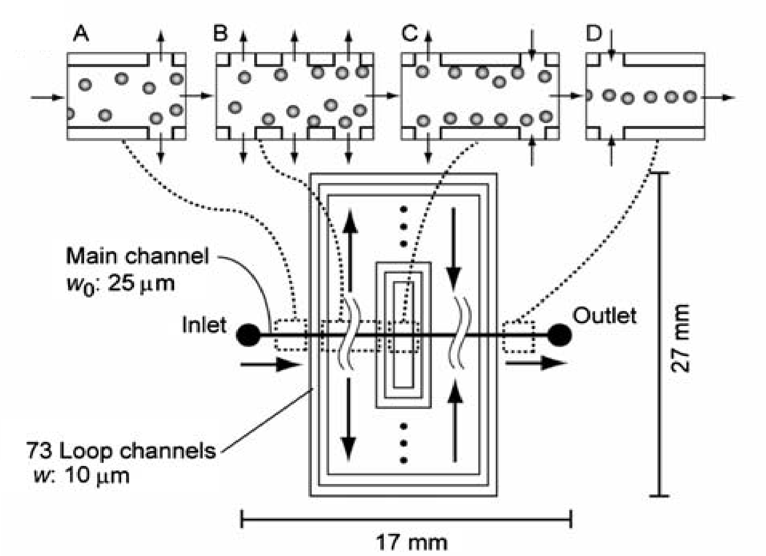

Device with multiple loop microchannels: Repeated splitting and re-injection of flow in the main channel from both sides gradually focuses the particles in the center.

Experimental: The main channel of the device has 146 (73 x 2) loop channels on its two sides (width 25 µm and 10 µm, respectively). $Q_1/Q_0 = 0.014 \Rightarrow w_1 \approx 1.75$ µm (*i.e.* particles ∅ > 3.5 µm would never flow into the loop channel). 85% of the initial flow is split from and then recombined into the mainstream.

100% of particles (Ø = 5 µm) were focused within a width of 2.5 µm around center line in the main channel.

Focusing efficiency was not affected by the flow speed, here 100 mm/s, high velocity! (The tracks of fluorescent particles look like lines).

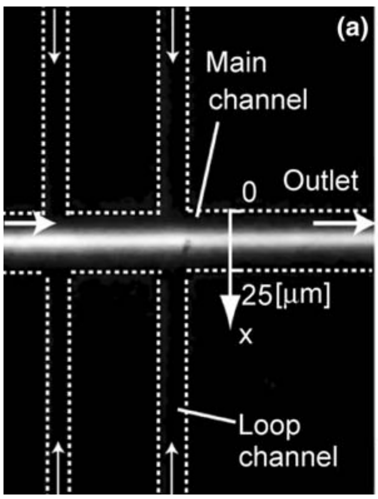

Fluorescent particles flowing near the outlet of the main channel.

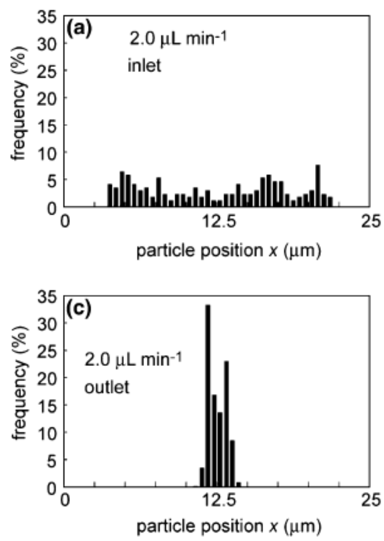

Particle position distributions at the inlet and outlet.

R. Aoki et al., Microfluid Nanofluid, 6, 571-576 (2009)

EPFL

3.3 Compliance (hydraulic capacitance)

Compliance due to compressible gas (e.g. air bubble in microchannel)

$$\boxed{C_{\mathrm{hyd}} \equiv -\frac{\mathrm{d}\mathcal{V}}{\mathrm{d}p}} \qquad (4.45)$$

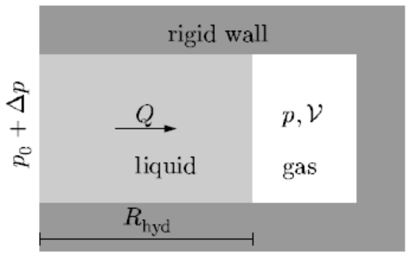

(Fig. 4.9)

$C_{\mathrm{hyd}} = p_0\mathcal{V}_0/p^2$ *using* $p\mathcal{V} = p_0\mathcal{V}_0$

$$Q(t) = -\partial_t \mathcal{V} = -(\partial_p \mathcal{V})\partial_t p = C_{\mathrm{hyd}}\partial_t p$$

$$(p_0 + \Delta p) - p = R_{\mathrm{hyd}} Q = -R_{\mathrm{hyd}}\partial_t \mathcal{V} = R_{\mathrm{hyd}} C_{\mathrm{hyd}} \partial_t p$$

$$\boxed{p(t) = p_0 + \left(1 - e^{-t/\tau}\right)\Delta p, \quad \tau \equiv R_{\mathrm{hyd}} C_{\mathrm{hyd}}} \qquad (4.47)$$

Analogy to voltage drop on charging capacitor

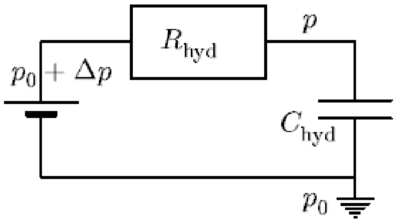

Equivalent electrical circuit

EPFL

Compliance due to elasticity of the channel wall (e.g. PDMS microchannels and valves, polymer tubes)

$$Q_1 = Q_2 + Q_c$$

$$Q_1 = (p_0 + \Delta p - p_c)/R_1$$

$$Q_2 = (p_c - p_0)/R_2$$

$$Q_c = -\partial_t \mathcal{V} = C_{\mathrm{hyd}}\partial_t p_c$$

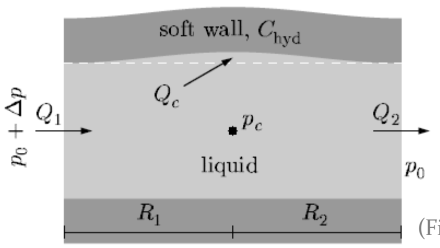

(Fig. 4.9)

$$\partial_t p_c = -\left(\frac{1}{\tau_1} + \frac{1}{\tau_2}\right)p_c + \left(\frac{1}{\tau_1} + \frac{1}{\tau_2}\right)p_0 + \frac{1}{\tau_1}\Delta p$$

with $\tau_1 = R_1 C_{\mathrm{hyd}}$ and $\tau_2 = R_2 C_{\mathrm{hyd}}$

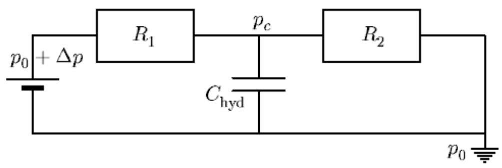

$$\boxed{p_c(t) = p_0 + \left(1 - e^{-\left[\tau_1^{-1} + \tau_2^{-1}\right]t}\right)\frac{\tau_2}{\tau_1 + \tau_2}\Delta p} \qquad (4.49)$$

Analog to voltage drop on capacitor charging through a voltage divider.

(Fig. 4.10)

EPFL

3.4 Microfluidic devices based on elastomeric components

Example 1: PDMS on-chip valves for microfluidic large-scale integration

Multilayer soft lithography enabled active microfluidic systems with monolithic PDMS valves and peristaltic pumps.

⇨ *Microfluidic large-scale integration* refers to microfluidic chips with thousands of valves, chambers and control components.

⇨ *Goal*: Replacing conventional methods for fluidic automation (*e.g.* pipetting robots), in particular for biological and biochemical applications.

(see for example: *J. Melin and S. Quake, Annu. Rev. Biophys. Biomol.* Struct., 36:213–31, 2007)

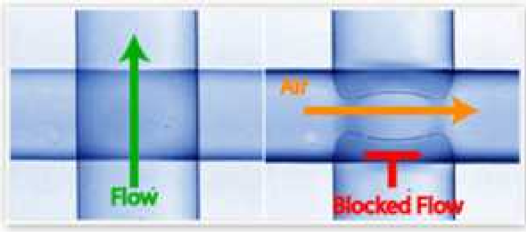

"Quake Valves" based on two crossing PDMS channels, *i.e.* a fluidic channel and a control channel, in open and closed state.

https://www.fluidigm.com/about/technology

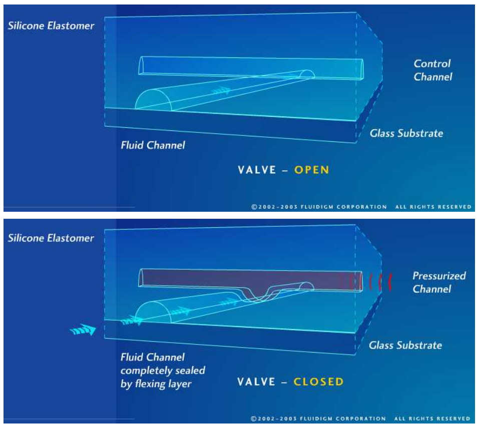

EPFL

Microfluidic large-scale integration

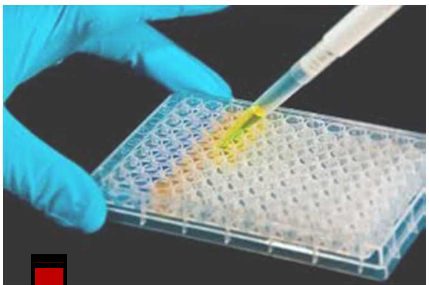

T. Thorson et al. , SCIENCE, VOL 298, 580-584, 2002

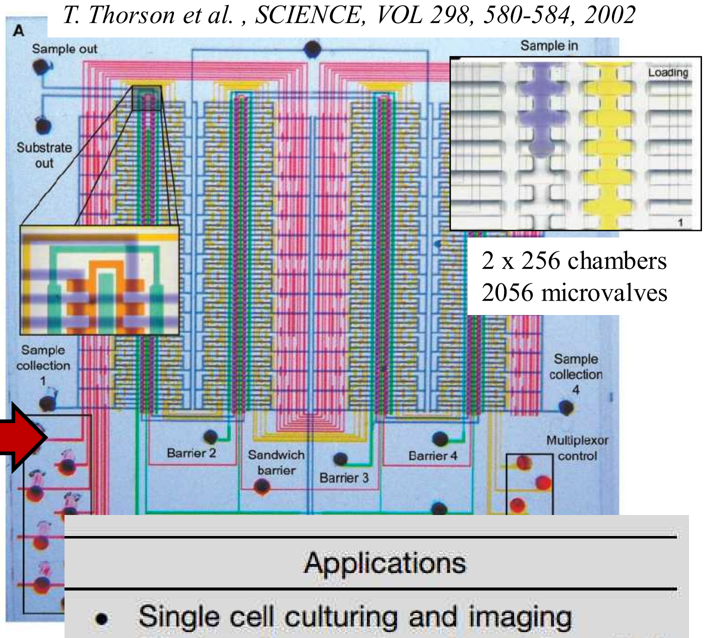

Applications

- Single cell culturing and imaging
- Single cell genomic and protein analysis
- Cell microenvironmental interaction
- Protein synthesis and characterization
- Chemical and biological screening

I.E. Araci and P. Brisk, *Recent developments in microfluidic large scale integration*, Current Opinion in Biotechnology 2013, 25:60–68

Integrated bioprocessor chip for DNA purification

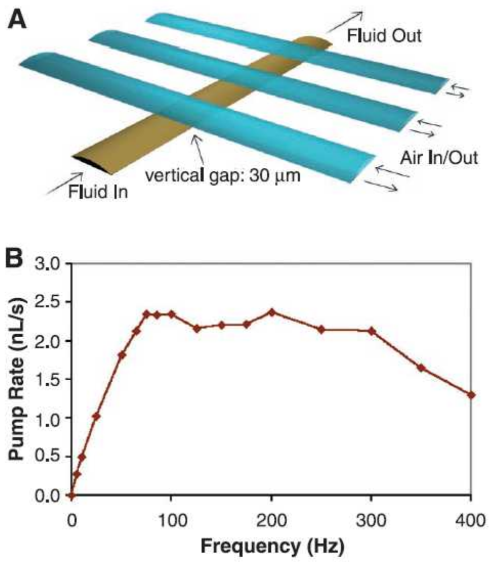

(A) 3D scale diagram of an elastomeric peristaltic pump. The channels are 100 µm wide and 10 µm high. (B) Pumping rate of a peristaltic micropump versus various driving frequencies.

*M.A. Unger et al., SCIENCE, **288**, 113-116 (2000)*

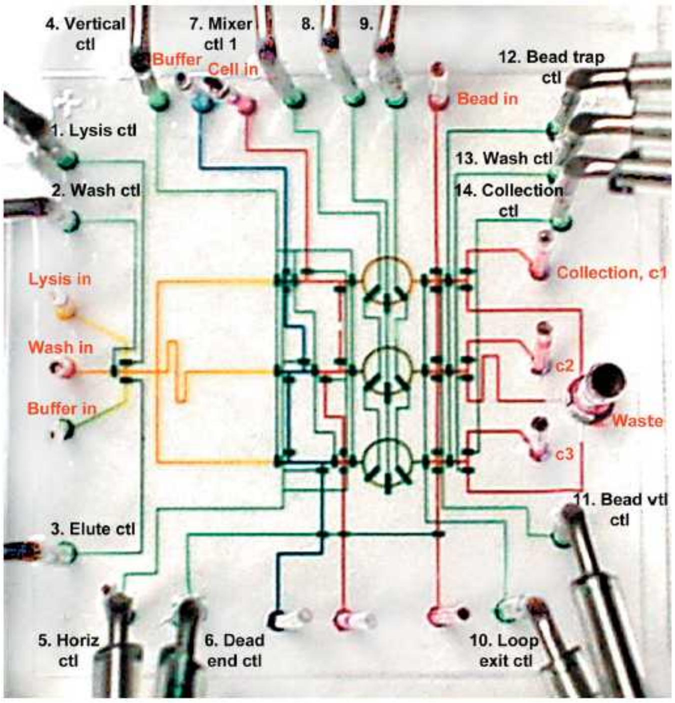

J.W. Hong, Nature Biotechnology, Vol. 22, p. 435 (2004)

Example 2: RC-tuned flow control

D. Leslie et al., Nature Physics 5, 231 - 235 (2009)

Fluid control in microfluidic devices is normally based on externally actuated valves. On-chip flow control would empower highly portable microfluidic tools.

⇨ *Possible new strategy for flow control*

- Fluidic networks with embedded deformable structures.
- Selective fluid transport / flow switching enabled by the frequency-dependent reponse of the circuit to a time-modulated external pressure source.
- This type of microfluidic circuit requires resistive and compliant structures, as well as check valves.
- Analogy to passive electrical *RC* circuits with diodes.

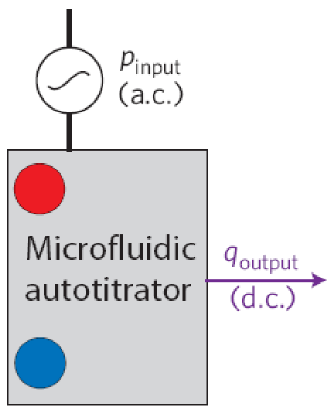

Principle of a microfluidic titrator: Controlled metering of two fluids by changing the actuation frequency ω of the pressure source (1 AC input controls the ratio of 2 solutions at the DC output).

Fluidic analogues to electrical circuit components

Fluidic capacitors

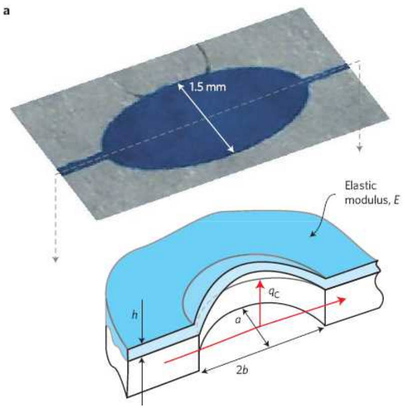

Fluidic capacitors are created by bonding deformable films (*e.g.* PDMS) over reservoirs placed in the network between fluidic channels (resistors) fabricated in glass.

$$C = \frac{\partial V}{\partial p} = \frac{\pi ab}{3k}$$

for circular shape

$$C = 16r^6/3Eh^3$$

Fluidic diodes

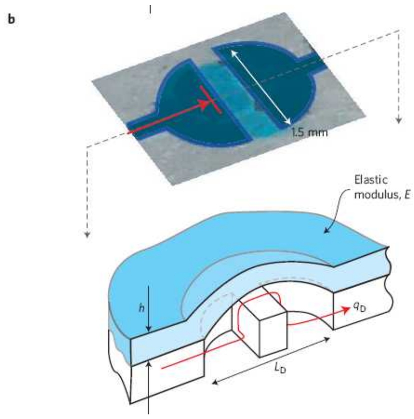

Fluidic diodes (check valves) are created by bonding deformable films around weirs that separate two channels in the network. The diode exhibits a nonlinear pressure-flow relationship. It opens if the internal pressure $p > p_{atm.}$

$$q \sim p^4 L_D^{11}/h^9 \qquad \text{(flow } q \text{ for } p > p_{atm})$$

D. Leslie et al., Nature Physics 5, 231 - 235 (2009)

Frequency-dependent fluidic network and equivalent circuit

Model circuit: RC branch with input *p(ω)*

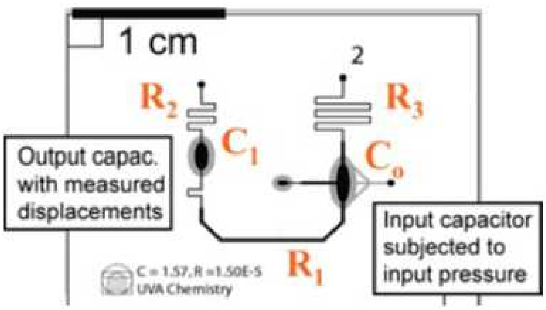

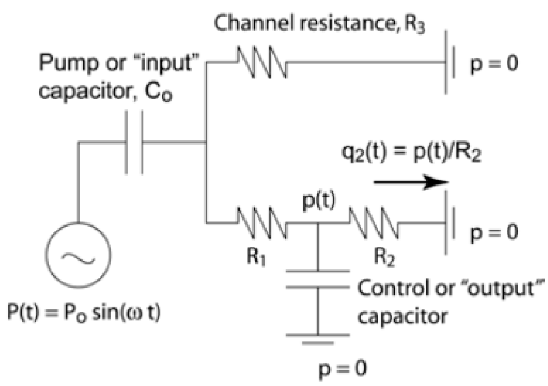

$$\left.\begin{array}{l} \Delta p = Rq \\ q = C\dot{p} \end{array}\right\} \quad \boxed{m\ddot{p}(t) + c\dot{p}(t) + kp(t) = C_o\dot{p}_{in}(t) = C_o p_o \omega \cos \omega t}$$

$$m = R_1 C,\ c = 1 + \frac{R_1}{R_3} + \frac{R_1}{R_2} + \frac{C}{C_o} \text{ and } k = \frac{1}{R_2 C_o}\left(1 + \frac{R_1}{R_3} + \frac{R_2}{R_3}\right)$$

D. Leslie et al., Nature Physics 5, 231 - 235 (2009)

Frequency response of a single RC branch (no diode)

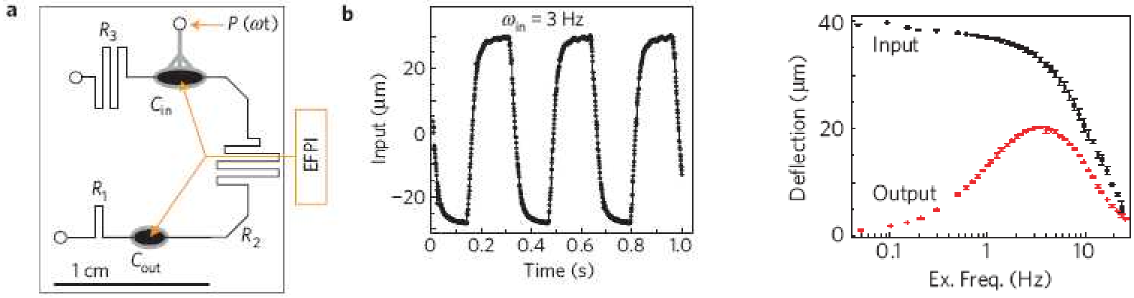

Model circuit: a) A square-wave pressure $p(\omega)$ is applied to the RC branch on C_{in}. The deflections of C_{in} and C_{out} are measured. b) Response (deflection) of C_{in} to $p(\omega t)$.

Frequency response at the input C_{in} (low-pass behavior) and at the output C_{out} (band-pass response).

$$\frac{\langle \delta_o \rangle}{\langle \delta_{in} \rangle} = \frac{\omega}{\sqrt{\beta^2 + (\alpha\omega)^2}}$$

(deflection $\delta \sim$ pressure p)

D. Leslie et al., Nature Physics 5, 231 - 235 (2009)

Resonant microfluidic circuit

Two RC branches with diodes are connected in parallel and driven by a single oscillatory pressure source. Each branch (band-pass) has a different frequency response.

⇨ Changing the frequency switches the flow output from one channel to the other.

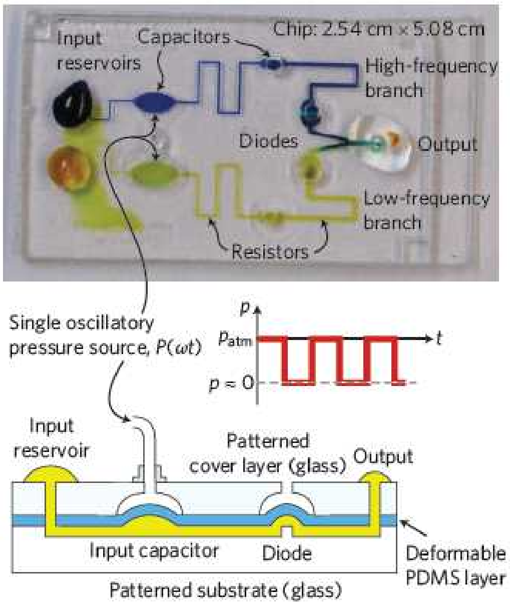

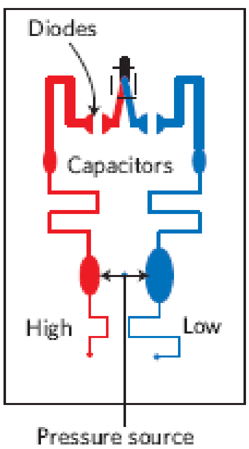

D. Leslie et al., Nature Physics 5, 231 - 235 (2009)

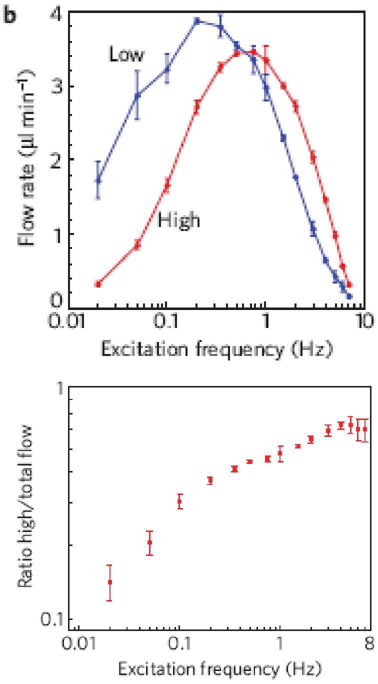

Top: Band-pass characteristics of the time-averaged output contributions from each branch of the network. *Bottom*: Ratio of the high-frequency branch as a fct. of total flow.

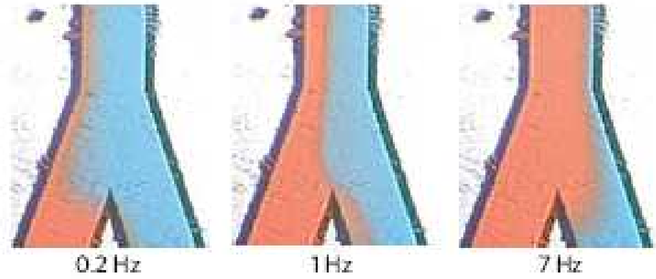

video

☹ large bandwidth, no “clean” switching !

D. Leslie et al., Nature Physics 5, 231 - 235 (2009)

Example 3: “Microfluidic electronics”

B. Mosadegh et al., Nature Physics, 6, 433-437 (2010)

A strategy to provide device-embedded flow switching and clocking functions: **Elastomeric components** form networks of fluidic gates that can spontaneously generate cascading and oscillatory flow output using only a constant flow of Newtonian fluids as the device input.

1) Check-valve as analogous to an electronic diode

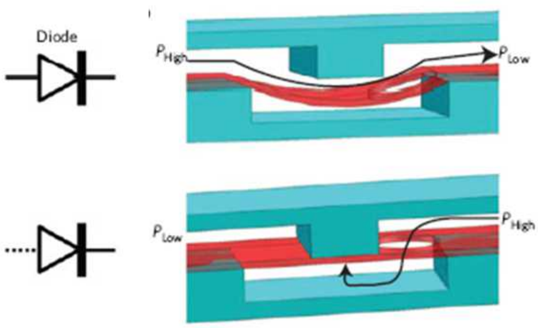

Cross-section schematic of the three-layer composite of a check-valve in open and closed state, respectively. The device consists of a PDMS membrane and two thicker layers.

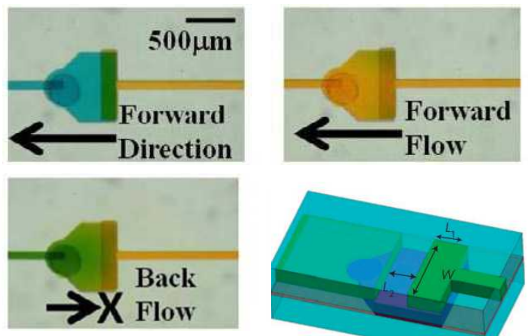

Check-valve operated with dyed solutions in open (forward flow) and closed state (back flow), respectively.

2) Switch-valve working as fluidic "field effect transistor"

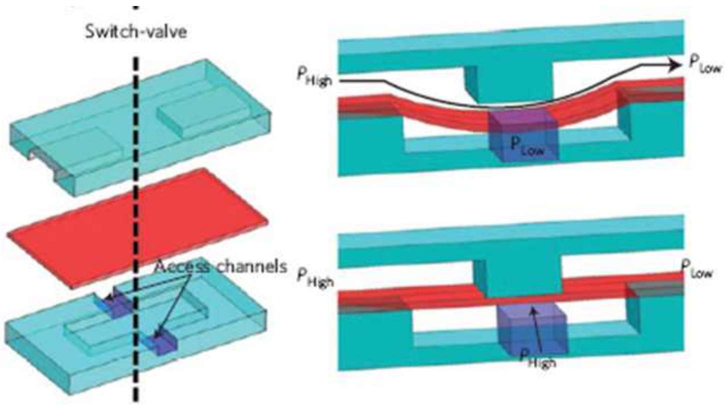

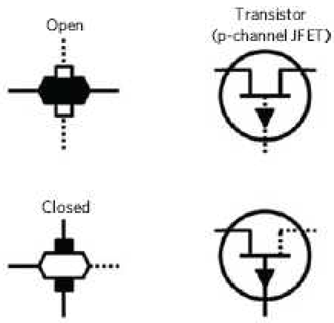

A three-layer composite of a switch-valve cross-section schematic in open and closed statee based on differential pressure, respectively.

Pressure controlled microfluidic switch-valve as analogous to FET transistor. The microfluidic component consists of two crossing channels.

B. Mosadegh et al., Nature Physics, 6, 433-437 (2010)

3) Interactive elastomeric components for oscillatory switching

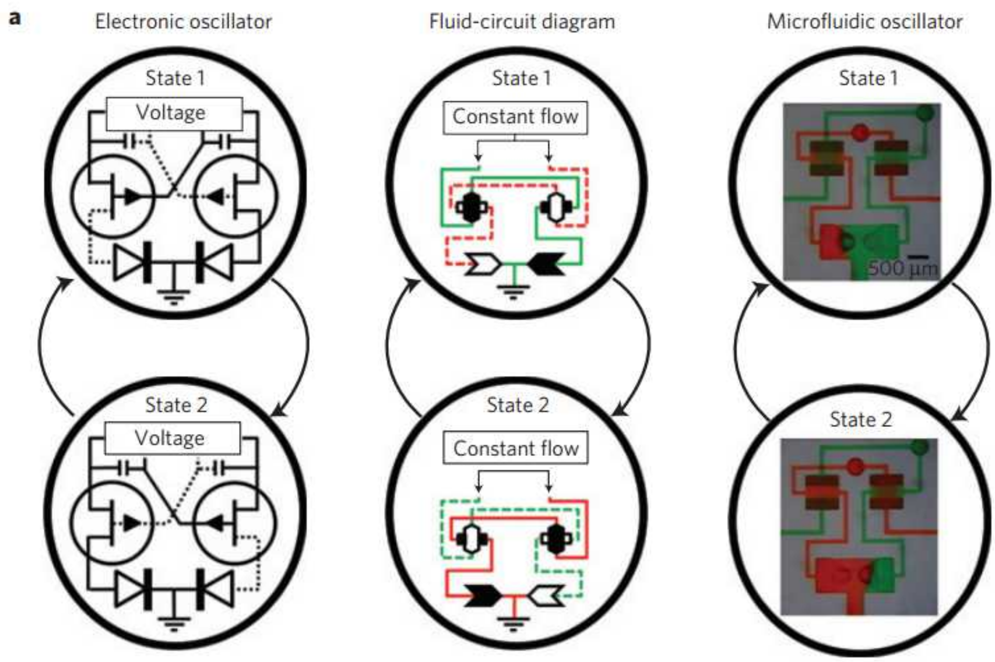

Comparison between a microfluidic oscillator and an electronic oscillator. The two states of a microfluidic oscillator automatically produce an alternating output flow between two distinct solutions being simultaneously infused at a constant rate (state 1 "green" flowing; state 2 "red" flowing, **see videos in the article SI**).

B. Mosadegh et al., Nature Physics, 6, 433-437 (2010)